

Research Article



Chemical Oscillators Hot Paper

How to cite: Angew. Chem. Int. Ed. 2025, 64, e202511413 doi.org/10.1002/anie.202511413

Experimentally Guided Iterative Parameter Estimation for Predictive Chemical Oscillator Models

Maëlle Le Cacheux, Luca E. Oddone, Sofiya A. Runikhina, Johanan Kootstra, Andreas Milias-Argeitis,* and Syuzanna R. Harutyunyan*

Abstract: Chemical oscillators are fundamental to dynamic processes in biology, from circadian rhythms to metabolic regulation, inspiring efforts to design synthetic analogues for use in responsive materials, autonomous systems, and molecular computing. However, creating robust and tunable synthetic oscillators remains a major challenge due to the inherent complexity and difficulty of identifying conditions that support sustained oscillations. We herein describe an iterative approach based on mathematical modeling and parameter estimation guided by live experimental data to accurately model the oscillating chemical network. Fitting a kinetic model to the whole chemical network proves considerably more effective and time-efficient than determining reaction rates individually and enables quick screening of various parameters. We apply this method to achieve sustained oscillations in flow when changing various aspects of our recently developed oscillating system, demonstrating its potential to facilitate the development and optimization of organic oscillators as well as offering a general framework for analyzing and optimizing complex synthetic CRNs.

Introduction

Nature is rich with nonlinear and dynamic processes that give rise to a wide range of complex behaviors. One of the most striking examples of such dynamics is oscillations, in which a system undergoes periodic changes in (thermodynamic) state over time. These oscillations are vital for life and play key roles in pattern formation, signal transduction, chemical responsiveness, and many others.^[1–8] Chemical oscillators, in which the concentration of one or more species varies periodically over time, are also typical examples of nonlinear dynamic behavior. Although the first synthetic chemical clock was already described in 1886 by Landolt, the first synthetic oscillator, the Belousov–Zhabotinsky (BZ) reaction, was discovered by serendipity in 1950 and still remains the best-known example of sustained chemical oscillations in a batch

(closed) system.^[9,10] The BZ and related reactions have been instrumental in advancing our understanding of nonlinear dynamics, emergent behavior, and pattern formation and have provided valuable insights into analogous mechanisms in living organisms.[11,12] Extensive efforts enabled the identification of the basic design principles required to construct oscillators. The first synthetic chemical oscillators were developed using a generic design strategy based on the cross-shaped phase diagram introduced by Boissonade and De Kepper in 1980.[13,14] This approach enabled the identification of oscillatory regimes without requiring detailed mechanistic models. In the 1990s, a more system-specific design method emerged, allowing for the construction of a wide range of pH oscillators based on simplified reaction schemes and mechanistic modeling.[15] At the heart of these systems lie chemical reaction networks (CRNs) that feature: autocatalysis, where a product accelerates its own formation, feedback inhibition, to suppress autocatalysis and "reset" the system, a triggering mechanism to allow state transitions, and a delay to introduce temporal separations between oscillatory cycles. These components collectively define a relaxation oscillator mechanism.^[16] To keep the system out of equilibrium, a constant energy inflow in the form of fresh reagent and outflow of the reaction mixture is implemented, often in a continuously stirred tank reactor (CSTR).

While these principles enabled the development of many inorganic oscillators, [17] very few oscillators based on organic molecules are known. [18-23] In contrast to their inorganic counterparts that often operate under harsh conditions, organic oscillators offer greater structural diversity, higher tunability, and compatibility with milder, more practical conditions. Achieving reliable and predictive control over organic oscillators is essential for advancing their utility, but, despite

Stratingh Institute for Chemistry, University of Groningen, Groningen 9747 AG, the Netherlands

E-mail: s.harutyunyan@rug.nl

Prof. A. Milias-Argeitis

Groningen Biomolecular Sciences and Biotechnology Institute, University of Groningen, Groningen 9747 AG, the Netherlands E-mail: a.milias.argeitis@rug.nl

Additional supporting information can be found online in the Supporting Information section

© 2025 The Author(s). Angewandte Chemie International Edition published by Wiley-VCH GmbH. This is an open access article under the terms of the Creative Commons Attribution-NonCommercial-NoDerivs License, which permits use and distribution in any medium, provided the original work is properly cited, the use is non-commercial and no modifications or adaptations are made.

^[*] M. Le Cacheux, L. E. Oddone, Dr. S. A. Runikhina, J. Kootstra, Prof. S. R. Harutyunyan

15213773, 2025. 38, Downloaded from https://onlinelibary.viley.com/doi/10.1002/anie.202511413 by Cochrane Austria, Wiley Online Library on [07/11/2025]. See the Terms and Conditions (https://onlinelibary.wiley.com/terms-and-conditions) on Wiley Online Library for rules of use; OA articles are governed by the applicable Creative Commons Licenses, and Conditions (https://onlinelibary.wiley.com/terms-and-conditions) on Wiley Online Library for rules of use; OA articles are governed by the applicable Creative Commons Licenses, and Conditions (https://onlinelibary.wiley.com/terms-and-conditions) on Wiley Online Library for rules of use; OA articles are governed by the applicable Creative Commons Licenses, and Conditions (https://onlinelibary.wiley.com/terms-and-conditions) on Wiley Online Library for rules of use; OA articles are governed by the applicable Creative Commons Licenses, and Conditions (https://onlinelibary.wiley.com/terms-and-conditions) on Wiley Online Library for rules of use; OA articles are governed by the applicable Creative Commons Licenses, and Conditions (https://onlinelibary.wiley.com/terms-and-conditions) on Wiley Online Library for rules of use; OA articles are governed by the applicable Creative Commons Licenses, and Conditions (https://onlinelibary.wiley.com/terms-and-conditions) on Wiley Online Library for rules of use; OA articles are governed by the applicable Creative Commons (https://onlinelibary.wiley.com/terms-and-conditions) on the applicable Creative Commons

well-established design frameworks, realizing sustained oscillations remains a major challenge. Oscillatory behavior only emerges within narrow regions of parameter space, making it difficult to determine the precise experimental conditions

under which it occurs.[24] Our group recently developed a modular catalytic organic oscillator, engineered for high tunability. To explore its behavior under varied conditions, we constructed a mathematical model that describes the chemical reactions in the CRN using rate constants measured from isolated reactions.^[21] This modeling approach, where the variables correspond directly to the starting materials in the system, differs from the phenomenological model approach introduced by Boissonade and De Kepper and requires the resulting model to have sufficient mechanistic and dynamical complexity to reproduce oscillating phenomena. Although this model reproduced the overall behavior of the CRN, it was not able to accurately predict oscillatory conditions when modifying the system or conditions. This is because CRNs are inherently complex, with each component directly or indirectly influencing others.[25,26] As a result, the reaction rates can be affected by not accounted side reactions, shifts in equilibria, and network-induced feedback, all of which differ substantially from behavior observed in isolation. Altering even a single component can ripple across the entire system, further widening the gap between measured and effective kinetics. Since models based on reaction rates determined in isolation do not take this into account, they describe the system in a state that does not exist under real operating conditions and consequently fail to accurately predict systemic behavior. This inaccuracy results in prolonged optimization times when making even minor adjustments, the need for numerous tedious kinetic studies, or, in the worst cases, complete failure to find the conditions for sustained oscillations. This problem is common for various types of designed oscillators and remains a significant hurdle, including in the model developed by our group.^[23] The main challenge, therefore, is to find the reaction rate constants that best describe the system in its oscillating regime. Unfortunately, most kinetics determination techniques require the isolation of the process followed, thus making them inherently flawed for our purposes.

Seeking a more effective approach for constructing a predictive mathematical model of our chemical oscillator, we turned to parameter estimation, a method to determine the combination of system parameter values that reproduces a set of experimental data. While this approach is widely used in dynamic systems modeling, [27-29] here we propose the use of parameter estimation as a design and optimization tool for chemical oscillators by embedding it within an iterative framework that combines model fitting to experimental data and in silico screening of initial conditions.

We first demonstrate how joint estimation of reaction rates outperforms traditional kinetic modeling to describe our oscillatory CRN. Using this method, we explore new operating conditions and show that it can identify initial conditions that support sustained oscillations at higher concentrations and at temperatures ranging from 60 to 90 °C. We then apply the same modeling framework to a variant of the system in which a component of the network is modified.

Without the need for exhaustive experimentation, parameter estimation enabled us to pinpoint conditions that support oscillations in this modified setup. Finally, we demonstrate how this approach allows the development of a de facto new oscillating system with a different secondary amine at the core of the CRN, requiring only two rounds of experiments and parameter estimation coupled with in silico screening of initial conditions.

Results and Discussion

The Fmoc-oscillator and Its Model

Well-mixed chemical systems can be modeled using ordinary differential equations (ODEs) that capture the concentration changes of each chemical species over time. [27,28] In the case of our Fmoc-oscillator, we previously constructed such a model based on the combination of the four main processes within the CRN, with an autocatalytic reaction at its core (Figure 1a).[23] Piperidine (1) is a base that is able to catalyze the cleavage of the Fmoc group. As a consequence, Fmoc-piperidine (2) can undergo autocatalytic deprotection, releasing more of 1 in the process, in a reaction of the form of $A + B \rightarrow 2B$ (reaction II). To obtain a single pulse in the concentration profile of 1, the latter needs to accumulate and then undergo depletion via additional reactions. To do so, an acetylating agent (4) reacts with 1 to form 6, lowering the concentration of 1 back to its initial state (reaction III). The system needs to be triggered by a small amount of base that cannot be inhibited (orthogonal to the other reactions within the CRN), and a tertiary amine (3) (reaction I) fulfills this role. Finally, in order to keep the system outof-equilibrium, the reagents need to be continuously supplied and the reaction mixture removed in a CSTR, while a faster acetylating agent (5) is used to delay the onset of the autocatalysis (reaction IV).

All processes described above follow second-order reaction rate laws (Figure 1a) in the prescribed conditions (in DMSO, at or > 60 °C). Therefore, the time evolution of 1 is described by the following ODE:

$$\frac{d[1]}{dt} = k_{\rm I} [3][2] + k_{\rm II}[1][2] - k_{\rm III}[1][4] - k_{\rm IV}[1][5]$$
 (1)

When the reactions of (1) take place inside a CSTR, the same kinetics apply, with an added space velocity term s_v to account for the inflow of fresh reagent (at concentration $[1]_0$) and the outflow of reaction mixture:

$$\frac{d[1]}{dt} = k_{\rm I} [3][2] + k_{\rm II}[1][2] - k_{\rm III}[1][4]$$

$$-k_{\rm IV}[1][5] + s_{\rm v}([1]_0 - [1])$$
(2)

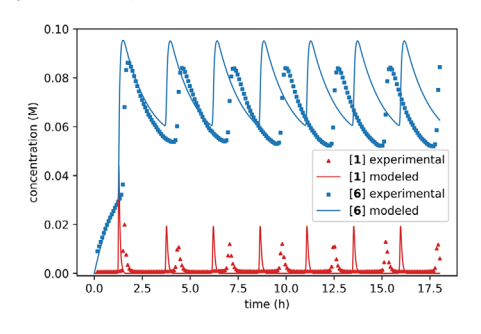
The remaining reactions of Figure 1 are modeled similarly, and their ODEs are provided in the Supporting Information.

15213773, 2025, 38, Downloaded from https://onlinelibrary.wiley.com/doi/10.1002/anie.202511413 by Cochrane Austria, Wiley Online Library on [07/11/2025]. See the Terms and Conditions (https://onlinelibrary.wiley.com/ems-and-conditions) on Wiley Online Library for rules of use; OA articles are governed by the applicable Creative Commons Licenses

a) Oscillator model

$\begin{array}{|c|c|c|}\hline \textbf{Reaction} & \textbf{Rate law} \\ \hline \textbf{Initiation (I)} & \frac{d[\mathbf{1}]}{dt} = k_I[3][2] \\ \hline \\ \textbf{Autocatalysis (II)} & \frac{d[\mathbf{1}]}{dt} = k_{II}[\mathbf{1}][2] \\ \hline \\ \textbf{Slow inhibition (III)} & \frac{d[\mathbf{1}]}{dt} = -k_{III}[\mathbf{1}][4] \\ \hline \\ \textbf{Fast inhibition (IV)} & \frac{d[\mathbf{1}]}{dt} = -k_{IV}[\mathbf{1}][5] \\ \hline \end{array}$

b) Model vs experiment: individual kinetic measurement



c) Model vs experiment: parameter estimation

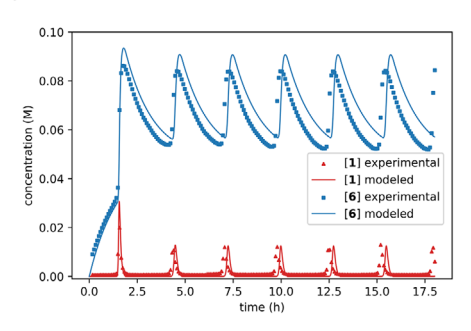


Figure 1. Kinetic description of the Fmoc-oscillator and model improvement via parameter estimation. Experimental data was measured by taking aliquots of the reaction mixture and measurements by GC-FID. a) All four main processes: I initiation reaction, II autocatalysis, III slow inhibition, and IV fast inhibition, and their related rate laws. b) Comparison of an oscillation experiment for conditions ([2]₀ = 0.1 M, [3]₀ = 0.005 M, [4]₀ = 1.8 M, [5]₀ = 0.03 M, $s_v = 1.00 \times 10^{-4} \text{ s}^{-1}$) to a model based on isolated reaction rate constants ($k_I = 2.02 \times 10^{-2} \text{ M s}^{-1}$, $k_{II} = 6.0 \times 10^{-1} \text{ M s}^{-1}$, $k_{III} = 2.8 \times 10^{-3} \text{ M s}^{-1}$, $k_{IV} = 2.2 \times 10^2 \text{ M s}^{-1}$). c) Comparison of the same experiment as in (b) to a model based on estimated apparent rate constants ($k_I = 1.75 \times 10^{-2} \text{ M s}^{-1}$, $k_{II} = 4.6 \times 10^{-1} \text{ M s}^{-1}$, $k_{III} = 4.5 \times 10^{-3} \text{ M s}^{-1}$, $k_{IV} = 5.0 \times 10^2 \text{ M s}^{-1}$).

Model Improvement via Parameter Estimation

To validate the model described above and demonstrate the benefit of jointly estimating apparent rate constants from full-system experimental data compared to inferring them from isolated reactions, we compared the model predictions under both estimation approaches to experimental data.

The system of ODEs is solved as initial value problems (IVP) using the *solve_ivp* package for Python from *scipy*.^[30] For parameter estimation with full-system data, the opensource software COPASI was used. COPASI makes use of an intuitive user interface to fit a kinetic model to experimental data and provides built-in optimization methods for parameter estimation.^[31] The constants $k_{\rm I}$, $k_{\rm II}$, and $k_{\rm III}$ (Figure 1a) were estimated, while k_{IV} was fixed at an arbitrarily high value of 500 M s⁻¹, as reaction IV is too fast to reliably identify the exact value (see Supporting Information, page 27). We then compared the predictions of our model with parameters obtained from individual reactions (Figure 1b) to those obtained from full-system data using parameter estimation (Figure 1c). The model using parameters inferred from isolated reactions does not fit well the experimentally obtained data, particularly the period and the amplitude of the concentration of 1, which is too high (Figure 1b). This is due to an overestimation of the autocatalysis rate constant. In contrast, the model with parameters obtained using parameter estimation represents the data very well (Figure 1c).

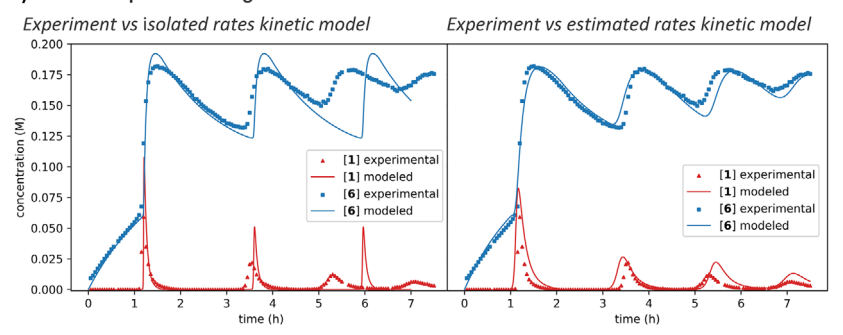
The differences between the reaction rate constants estimated individually and in full-system data can mostly be explained by the unmodeled effects that some components have on the system reactions. A prominent example of such an effect is *para*-nitrophenol (8), which is released as a product of the reaction between 1 and 5 and is acidic. This, in turn, slows down all base-catalyzed reactions performed by 1. Interestingly, this compound has little to no effect on the initiation rate constant as it remains close to 2×10^{-2} M s⁻¹ regardless of the method of rate determination and the experimental input. This is because the trigger 3 is not basic enough to be protonated by 8 in the tested conditions, which explains why it is not being deactivated and why the initiation rate constants are unaffected by the presence of 8.

First Case Study: Changing Component Concentrations

The difference between the two models is even more striking in an experiment in which the initial concentration [2]₀ was increased from 0.1 to 0.2 M (Figure 2a). The model with individually determined rates predicted this to lead to sustained oscillations, but the system converged to a stable spiral equilibrium with dampening oscillations. However, when applying parameter estimation to this new dataset and jointly determining the rate constants, the updated model correctly reproduced the experimental data, indicating that

15213773, 2025, 38, Downloaded from https://onlinelibrary.wiley.com/doi/10.1002/anie.202511413 by Cochrane Austria, Wiley Online Library on [07/11/2025]. See the Terms and Conditions (https://onlinelibrary.wiley.com/terms-and-conditions) on Wiley Online Library for rules of use; OA articles are governed by the applicable Creative Commons License

a) Model comparison for higher initial concentration of 2



b) Model prediction from estimated rates and experimental verification

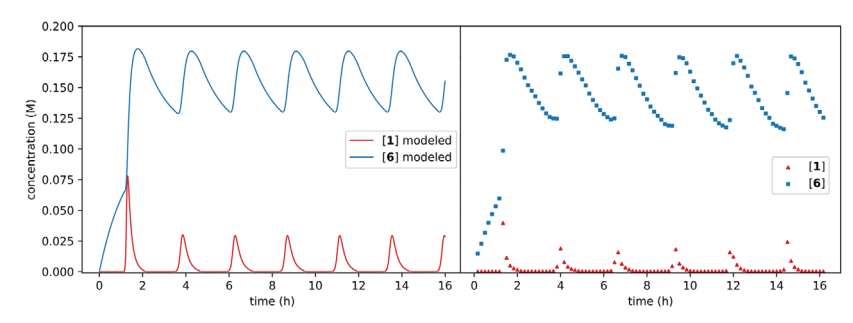


Figure 2. Study of the reported conditions using parameter estimation and optimization to sustain oscillations in higher initial concentration of 2. Experimental data was measured by taking aliquots of the reaction mixture and measurements by GC-FID. a) Model comparison for higher initial concentration of 2 ([2]₀ = 0.2 M, [3]₀ = 0.005 M, [4]₀ = 1.8 M, [5]₀ = 0.060 M, $s_v = 1.0 \times 10^{-4} \text{ s}^{-1}$) using isolated reaction rate constants ($k_1 = 2.02 \times 10^{-2} \text{ M s}^{-1}$, $k_{11} = 6.0 \times 10^{-1} \text{ M s}^{-1}$, $k_{11} = 2.8 \times 10^{-3} \text{ M s}^{-1}$, $k_{1V} = 2.2 \times 10^2 \text{ M s}^{-1}$) (left) and estimated apparent rate constants ($k_1 = 2.36 \times 10^{-2} \text{ M s}^{-1}$), $k_{11} = 1.0 \times 10^{-1} \text{ M s}^{-1}$, $k_{111} = 1.07 \times 10^{-3} \text{ M s}^{-1}$, $k_{1V} = 5.0 \times 10^2 \text{ M s}^{-1}$) (right). b) Model prediction of sustained oscillations using estimated apparent rate constants in tuned initial conditions ($k_1 = 2.36 \times 10^{-2} \text{ M s}^{-1}$), $k_{11} = 1.0 \times 10^{-1} \text{ M s}^{-1}$, $k_{111} = 1.07 \times 10^{-3} \text{ M s}^{-1}$, $k_{112} = 1.07 \times 10^{-2} \text{ M s}^{-1}$) (left) and the experimental verification (right).

the estimated rate constants better describe the system behavior under these new conditions.

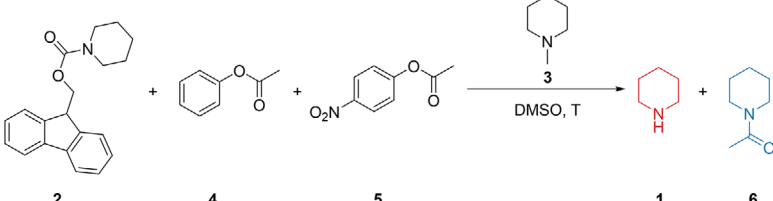
Since the observed spiral equilibrium suggested that oscillations could be achievable, we set out use these estimated rate constants to predict suitable starting conditions by screening in silico different initial conditions while keeping [2]₀ fixed at 0.2 M. According to the updated model, slightly increasing the initial concentration of 5 from 0.06 to 0.065 M would allow the system to reach a stable oscillating regime, which was subsequently confirmed experimentally (Figure 2b).

Overall, besides providing new conditions for sustained oscillations in a setting where our previous strategy had failed, the model based on parameter estimation revealed a new regime of oscillations, enabling the release of 1 at higher amounts, from 12 mM (Figure 1b) up to 25 mM in this work (Figure 2b), increasing the control we have over the system.

Second Case Study: Changing the Temperature

Controlling the temperature in the chemical system is of prime interest, as it allows for finer tuning of the oscillations. However, as the temperature changes, all reaction rate constants of the system change as well, making it hard to anticipate which operating regime might maintain stable sustained oscillations. Our original system was run in DMSO at 68 °C.^[23] Here we show that, with changes in the initial conditions, we can reach sustained oscillations at 60, 80, and 90 °C. To estimate the new apparent rate constants and fine-tune the initial conditions, we ran flow experiments at different temperatures with the initial conditions of the original system. At 60 °C, the chemical system displayed dampened oscillations, and we used this response to estimate the new apparent rate constants of our model. The updated model predicted that a small change in slow inhibitor 4

15213773, 2025, 38, Downloaded from https://onlinelibrary.wiley.com/doi/10.1002/anie.202511413 by Cochrane Austria, Wiley Online Library on [07/11/2025]. See the Terms and Conditions (https://onlinelibrary.wiley.com/terms-and-conditions) on Wiley Online Library for rules of use; OA articles are governed by the applicable Creative Commons License



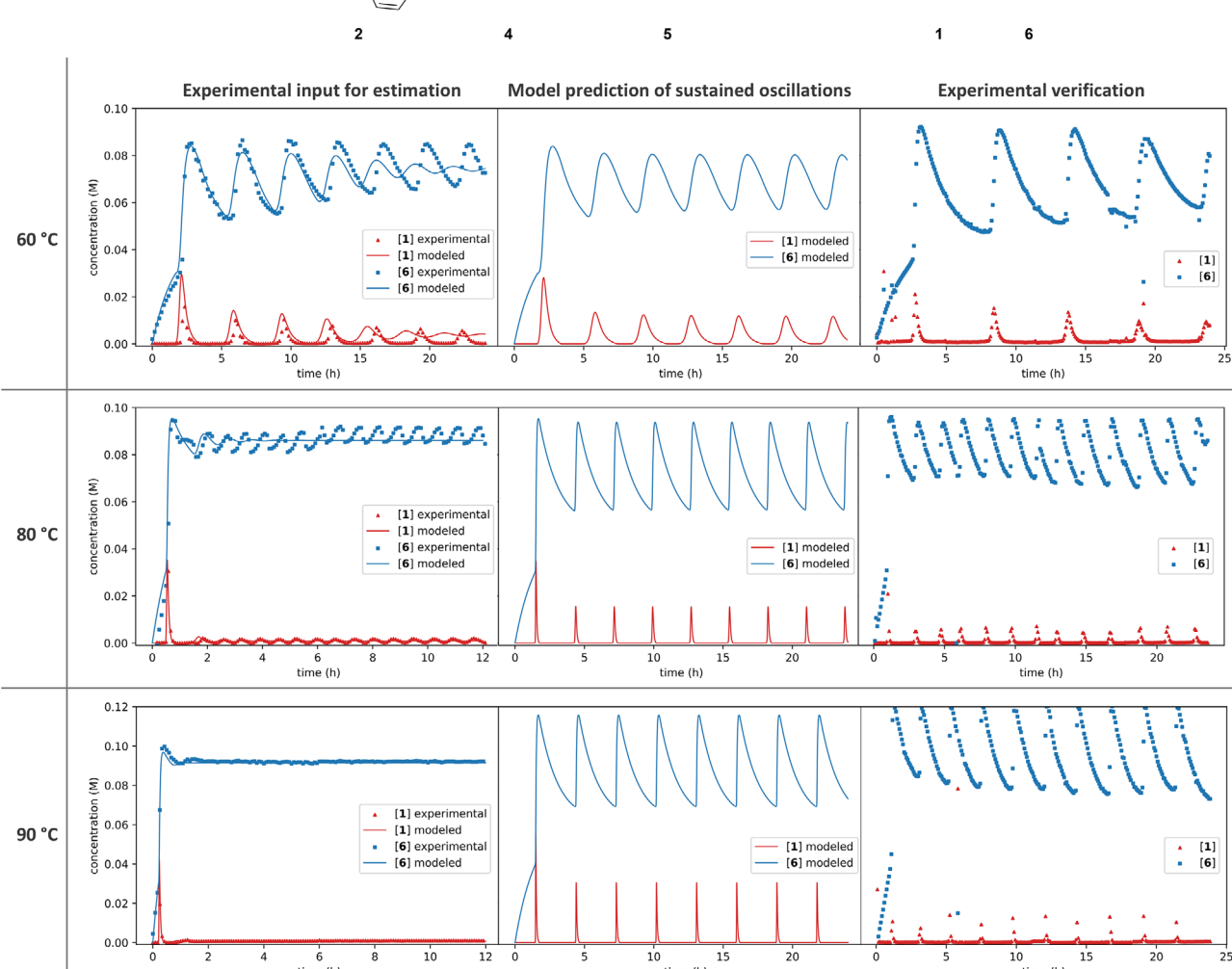


Figure 3. Optimization toward sustained oscillations at 60, 80, and 90 °C. Experimental data was measured by taking aliquots of the reaction mixture and measurements by GC-FID. Experimental input initial conditions ([2]₀ = 0.1 M, [3]₀ = 0.005 M, [4]₀ = 1.8 M, [5]₀ = 0.03 M, $s_v = 1.00 \times 10^{-4} \text{ s}^{-1}$). At 60 °C (rates estimated: $k_l = 1.6 \times 10^{-2} \text{ M s}^{-1}$, $k_{ll} = 7.1 \times 10^{-2} \text{ M s}^{-1}$, $k_{lll} = 6.6 \times 10^{-4} \text{ M s}^{-1}$, $k_{lV} = 5.0 \times 10^2 \text{ M s}^{-1}$) initial conditions picked ([2]₀ = 0.1 M, [3]₀ = 0.005 M, [4]₀ = 1.9 M, [5]₀ = 0.03 M, $s_v = 1.00 \times 10^{-4} \text{ s}^{-1}$), at 80 °C (rates estimated: $k_l = 4.5 \times 10^{-2} \text{ M s}^{-1}$, $k_{ll} = 5.1 \times 10^{-1} \text{ M s}^{-1}$, $k_{lll} = 3.7 \times 10^{-3} \text{ M s}^{-1}$, $k_{lV} = 5.0 \times 10^2 \text{ M s}^{-1}$, initial conditions picked: [2]₀ = 0.1 M, [3]₀ = 0.002 M, [4]₀ = 1.8 M, [5]₀ = 0.03 M, $s_v = 1.00 \times 10^{-4} \text{ s}^{-1}$), at 90 °C (rates estimated: $k_l = 1.0 \times 10^{-1} \text{ M s}^{-1}$, $k_{ll} = 9.4 \times 10^{-1} \text{ M s}^{-1}$, $k_{lll} = 4.1 \times 10^{-3} \text{ M s}^{-1}$, $k_{lV} = 5.0 \times 10^2 \text{ M s}^{-1}$, initial conditions picked: [2]₀ = 0.12 M, [3]₀ = 0.001 M, [4]₀ = 1.6 M, [5]₀ = 0.04 M, $s_v = 1.00 \times 10^{-4} \text{ s}^{-1}$).

(from 1.8 to 1.9 M) would help reach stable oscillations over 24 h, which was verified experimentally (Figure 3, 60 °C). At 80 °C, the chemical system displayed sustained oscillations with very short period and amplitude. Using these experimental data to estimate new apparent rate constants for our model, we found that reducing the amount of 3 from 0.005 to 0.002 M increased the amplitude and delay period between piperidine peaks (Figure 3, 80 °C). Finally, at 90 °C, the chemical system reached an equilibrium in less than 2 h with an extremely short lag phase. By repeating the apparent rate constant estimation, we found new initial

conditions for sustained oscillations (Figure 3, 90 $^{\circ}$ C). In summary, the method allowed us to successfully induce sustained oscillations in our chemical system in a range of temperatures.

Third Case Study: Changing the Slow Inhibitor

These promising results suggested that it may be possible to use the parameter estimation-based model to find conditions leading to sustained oscillations when greater changes are

15213773, 2025, 38, Downloaded from https://onlinelibrary.wiley.com/doi/10.1002/anie.202511413 by CochraneAustria, Wiley Online Library on [07/11/2025]. See the Terms and Conditions (https://onlinelibrary.wiley.com/terms

-and-conditions) on Wiley Online Library for rules of use; OA articles are governed by the applicable Creative Commons License

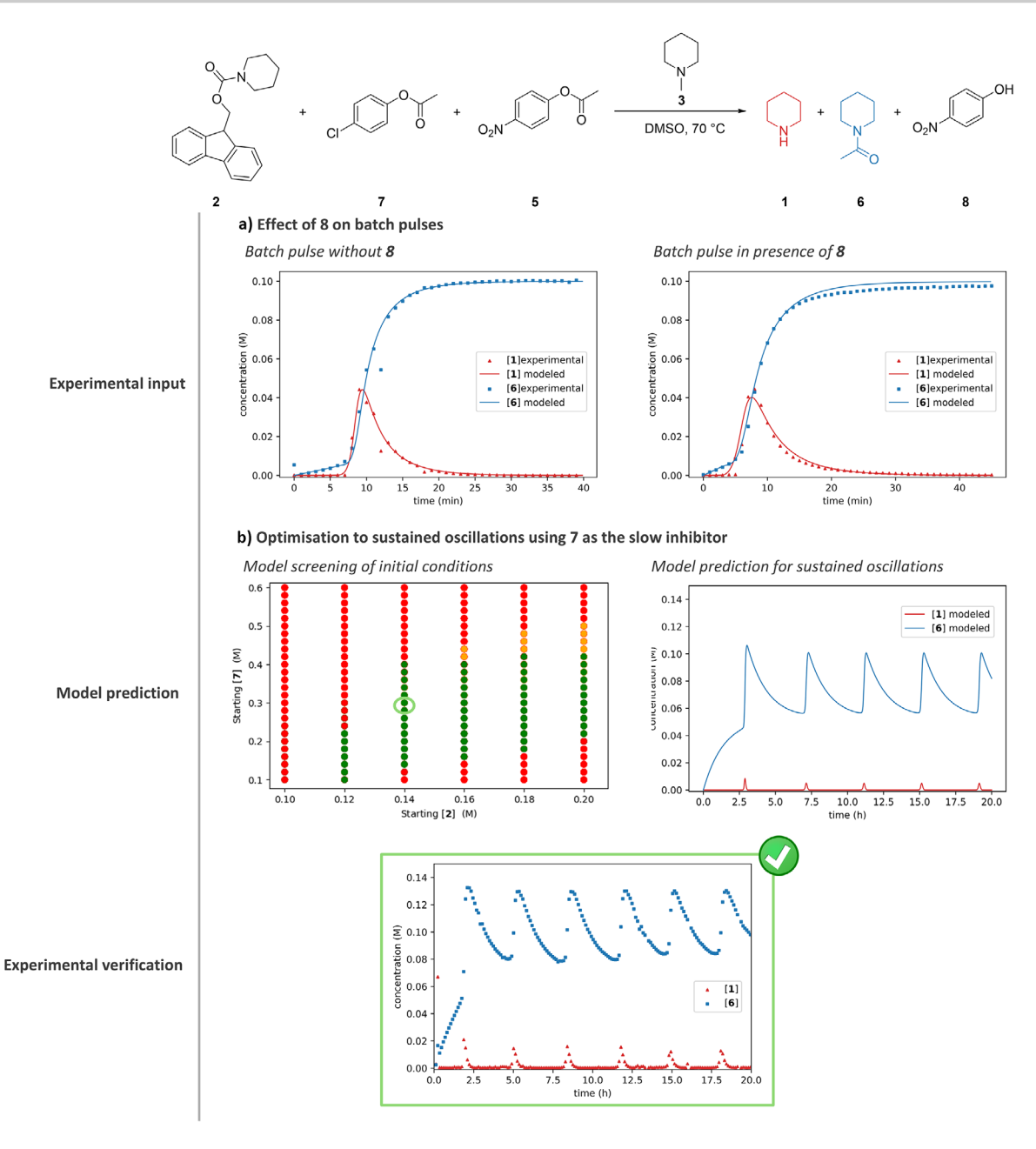


Figure 4. Optimization from a batch pulse to sustained oscillations using 7 as the slow inhibitor. Experimental data was measured by taking aliquots of the reaction mixture and measurements by GC-FID. a) Effect of para-nitrophenol 8 on batch pulses and the corresponding parameter fit. Initial conditions without 8 ([2]₀ = 0.1 M, [3]₀ = 0.005 M, [7]₀ = 0.15 M, [5]₀ = 0.005 M, $s_v = 0 s^{-1}$) ($k_l = 2.5 \times 10^{-2} \text{ M s}^{-1}$, $k_{lll} = 5.1 \times 10^{-1} \text{ M s}^{-1}$, $k_{lll} = 5.1 \times 10^{-1} \text{ M s}^{-1}$, $k_{lll} = 5.6 \times 10^{-2} \text{ M s}^{-1}$, $k_{lll} = 5.0 \times 10^{2} \text{ M s}^{-1}$) (left) and in the presence of 8 ([8]₀ = 0.025 M) ($k_l = 4.6 \times 10^{-2} \text{ M s}^{-1}$, $k_{ll} = 3.5 \times 10^{-1} \text{ M s}^{-1}$, $k_{lll} = 5.6 \times 10^{-2} \text{ M s}^{-1}$, $k_{lll} = 5.0 \times 10^{2} \text{ M s}^{-1}$) (right). b) Optimization to sustained oscillations using 7 as the slow inhibitor. Conditions picked after model screening of initial conditions for sustained oscillations ($k_l = 2.5 \times 10^{-2} \text{ M s}^{-1}$, $k_{lll} = 3.5 \times 10^{-1} \text{ M s}^{-1}$, $k_{lll} = 5.6 \times 10^{-2} \text{ M s}^{-1}$, $k_{lll} = 5.6 \times 10^{-2} \text{ M s}^{-1}$, initial conditions: [2]₀ = 0.14 M, [3]₀ = 0.003 M, [7]₀ = 0.34 M, [5]₀ = 0.045 M, $s_v = 1.25 \times 10^{-4} \text{ s}^{-1}$), model prediction for the conditions picked and its experimental verification.

introduced to the original system. To test this, we changed the slow inhibitor 4, one of the key components of the CRN, to a faster acylating reagent: *para*-chlorophenyl acetate (7). We made this change expecting that the chloride substituent would increase the reactivity of the acetylating agent compared to 4, allowing us to work at a lower concentration of slow inhibitor. In turn, this would change not only the reagent but also the polarity of the reaction mixture.

Initial data for estimating the rate constants for the new chemical system was generated using batch experiments, as they require less material, lower reaction times, simpler setups, simpler tuning of conditions and lower analysis time compared to flow experiments. To provide sufficiently informative data for parameter estimation, we designed a proper pulse experiment in batch conditions, displaying a clear lag phase, exponential growth of 1 and subsequent

15213773, 2025, 38, Downloaded from https://onlinelibrary.wiley.com/doi/10.1002/anie.202511413 by Cochrane Austria, Wiley Online Library on [07/11/2025]. See the Terms and Conditions (https://onlinelibrary.wiley.com/doi/10.1002/anie.202511413 by Cochrane Austria, Wiley Online Library on [07/11/2025]. See the Terms and Conditions (https://onlinelibrary.wiley.com/doi/10.1002/anie.202511413 by Cochrane Austria, Wiley Online Library on [07/11/2025]. See the Terms and Conditions (https://onlinelibrary.wiley.com/doi/10.1002/anie.202511413 by Cochrane Austria, Wiley Online Library on [07/11/2025]. See the Terms and Conditions (https://onlinelibrary.wiley.com/doi/10.1002/anie.202511413 by Cochrane Austria, Wiley Online Library on [07/11/2025]. See the Terms and Conditions (https://onlinelibrary.wiley.com/doi/10.1002/anie.202511413 by Cochrane Austria, Wiley Online Library on [07/11/2025]. See the Terms and Conditions (https://onlinelibrary.wiley.com/doi/10.1002/anie.202511413 by Cochrane Austria, Wiley Online Library on [07/11/2025]. See the Terms and Conditions (https://onlinelibrary.wiley.com/doi/10.1002/anie.202511413 by Cochrane Austria, Wiley Online Library on [07/11/2025]. See the Terms and Conditions (https://onlinelibrary.wiley.com/doi/10.1002/anie.202511413 by Cochrane Austria, Wiley Online Library on [07/11/2025]. See the Terms and Conditions (https://onlinelibrary.wiley.com/doi/10.1002/anie.202511413 by Cochrane Austria, Wiley Online Library on [07/11/2025]. See the Terms and Conditions (https://onlinelibrary.wiley.com/doi/10.1002/anie.202511413 by Cochrane Austria, Wiley Online Library on [07/11/2025]. See the Terms and Conditions (https://onlinelibrary.wiley.com/doi/10.1002/anie.202511413 by Cochrane Austria, Wiley Online Library on [07/11/2025]. See the Terms and Conditions (https://onlinelibrary.wiley.com/doi/10.1002/anie.202511413 by Cochrane Austria, Wiley Online Library on [07/11/2025]. See the Terms and Conditions (https://onlinelibrary.wiley.com/doi/10.1002/anie.202511413 by Cochrane Austria, Wiley

s-and-conditions) on Wiley Online Library for rules of use; OA articles are governed by the applicable Creative Commons License

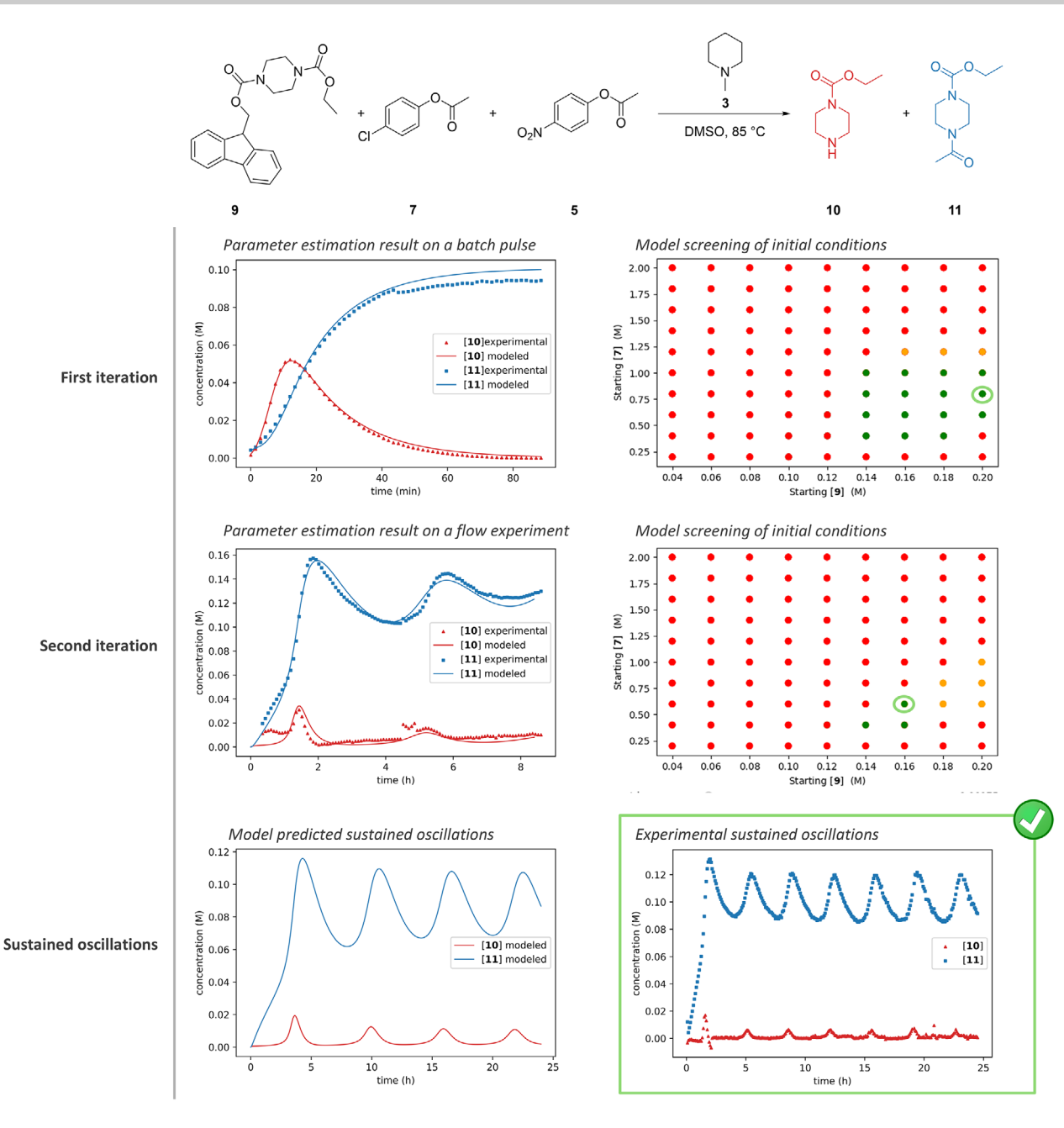


Figure 5. Optimization toward sustained oscillation using 10 as a new secondary amine. Experimental data was measured by taking aliquots of the reaction mixture and measurements by GC-FID. First iteration: parameter estimation results from a batch pulse ([9]₀ = 0.1 M, [3]₀ = 0.005 M, [7]₀ = 0.3 M, [5]₀ = 0.005 M, $s_v = 0$ s⁻¹) and model screening for initial conditions. Second iteration: parameter estimation results from a damped flow experiment ($k_1 = 2.3 \times 10^{-2}$ M s⁻¹, $k_{11} = 3.6 \times 10^{-2}$ M s⁻¹, $k_{111} = 2.2 \times 10^{-3}$ M s⁻¹, $k_{1V} = 1.8 \times 10^{-1}$ M s⁻¹, initial conditions: [9]₀ = 0.2 M, [3]₀ = 0.001 M, [7]₀ = 0.8 M, [5]₀ = 0.05 M, $s_v = 1.25 \times 10^{-4}$ s⁻¹) and model screening for initial conditions. Sustained oscillations: model predicted oscillations and experimental verification ([9]₀ = 0.16 M, [3]₀ = 7.5 × 10⁻⁴ M, [7]₀ = 0.6 M, [5]₀ = 0.05 M, $s_v = 1.25 \times 10^{-4}$ s⁻¹.

inhibition (Figures 4a (left) and S2). We used this data to estimate the apparent rate constants in the network, but parameters measured from batch pulses are not expected to accurately predict the behavior of the CRN in flow. In particular, the role of the fast inhibitor differs greatly between batch and flow experiments. In batch, the fast inhibitor controls the length of the initial lag phase and is completely consumed. Therefore, its only role is to control when the pulse will occur with little to no impact on the pulse itself.

In a flow experiment, on the other hand, the fast inhibitor is continuously added, altering the dynamic behavior of the system. Thus, in flow conditions a much higher concentration is needed than in batch. With a higher amount of the fast inhibitor 5 reacting in solution comes a higher amount of *para*-nitrophenol 8, which significantly slows down most processes. To take this effect into account and to approximate flow conditions, batch pulses can be performed with an initial amount of *para*-nitrophenol 8 (Figure 4a, right). In the



Research Article



absence of **8**, the estimated values of $k_{\rm II}$ and $k_{\rm III}$ are 5. 1 \times 10⁻¹ and 7.6×10^{-2} M s⁻¹, respectively, while in the presence of **8**, these values are 3.5×10^{-1} and 5.6×10^{-2} M s⁻¹. As expected, we observed that the autocatalysis and the inhibition rates are slower in the presence of 8. However, the observed lag phase was much shorter compared to experiments without 8, probably due to traces of water in our para-nitrophenol, leading to hydrolysis of 5. Expecting this effect would lead to an overestimation of the initiation rate constant $k_{\rm I}$, we used the $k_{\rm I}$ value obtained from the batch experiment without 8 as an approximation of the trigger rate of the system, while using the $k_{\rm II}$ and $k_{\rm III}$ values from the batch experiment in the presence of 8 (Figure 4b). Using the apparent rate constants described above, we then simulated the kinetic model for a large number of initial conditions to identify those initial conditions for which the system converges to a stable limit cycle (i.e., sustained oscillations) (see Supporting Information, page 25). To verify the model a set of conditions were picked in the range predicted to support sustained oscillations (see Supporting Information, page 25 for the criteria used to pick the conditions), and the chemical system did indeed display sustained oscillations (Figure 4b). With this new setup, we were able to successfully reduce the amount of slow inhibitor needed, from the 1.8 M of 4 previously reported to only 0.34 M of 7 in this work.^[23]

Fourth Case Study: Changing the Secondary Amine

The most challenging modification of our chemical system amounts to changing the amine at its core. This is the only component taking part in every reaction, equating this change to the de facto creation of a new chemical oscillator. To further test our modeling-based approach for generating oscillatory systems, we chose carbethoxypiperazine (10), an amine known for its connection to potential anticancer prodrugs, [32,33] as an alternative to piperidine (1). The presence of a stable carbamate group is also of interest for further applications due to its synthetic tunability. To highlight the iterative aspect of our method and to remove the need for an arbitrary additional component (addition of 8 in batch pulses in the case study previously described) in the experiment design, we used a single batch experiment with no additives as experimental input for the estimation of apparent rate constants. Similar to the third case study, an informative batch experiment needs to exhibit a clear lag phase, exponential growth of 10 and subsequent return to 0 M. The first attempt at a batch pulse led to incomplete conversion of 9 and the concentration of 10 did not go back to 0 M at 60 °C using 4 as slow inhibitor. The slower autocatalysis and low inhibition rates compared to piperidine 1 can be explained by lower nucleophilicity and p K_aH of 10 compared to 1. To obtain a proper pulse, we increased the temperature to 85 °C to increase the rate of autocatalysis and used 7 to speed up the slow inhibition, maintaining these changes for all further experiments using 10 (Figure S4). From this batch pulse, we estimated apparent rate constants and built a model which we then used to scan for initial conditions from which the chemical system converges to a stable limit cycle in a flow experiment (Figure 5, first iteration). However, when we picked a set of initial conditions in the range predicted by the model, the system converged to a stable spiral instead of a limit cycle. Differences between batch and flow conditions are the most likely culprits for this lack of predictive power of this first model. However, using this unsuccessful flow experiment as a new dataset to re-estimate the rate constants of the model offered a new opportunity to search for initial conditions leading to sustained oscillations in silico. When we picked a new set of initial conditions within the range of the new model predictions, we were able to achieve sustained oscillations using amine 10 at the core of the CRN (Figure 5), thereby completing the development of this new chemical oscillator.

Conclusion

In this work, we showed that joint parameter estimation enables efficient identification of sustained oscillations in the Fmoc oscillator across diverse conditions, offering a robust tool for predictive design of dynamic chemical systems. Starting from the original system configuration, we could achieve piperidine oscillations with a higher amplitude and a peak of 25 mM by changing the initial concentration of two components. Next, we obtained sustained oscillations in temperatures ranging from 60 to 90 °C. We were also able to replace one of the key components of the CRN, the slow inhibitor, with a faster reagent, while maintaining the oscillations. Finally, we developed a de facto new oscillating system with a different amine at its core and achieved sustained oscillations in only two iterations of parameter estimation followed by model predictions.

As these results demonstrate, mathematical modeling of chemical oscillators followed by experimentally guided parameter estimation based on full-system data is a highly promising approach for designing and optimizing the chemical system under various conditions. It is also highly accessible for the optimization of any synthetic CRN, as it relies on open-source computing tools such as COPASI and Python. Our method is limited by the accuracy of the mechanistic model and the apparent rate constants. While iterative parameter estimation can largely compensate for inaccuracies in the mechanistic model of the oscillatory CRN, these inaccuracies can limit the predictive accuracy of the model if they become too large. To facilitate the design of dynamic CRNs in the absence of precise mechanistic information, our method could be coupled to recent advances in the development of black-box dynamical models using machine learning techniques. Thanks to its low computational cost, parameter estimation can be used to fit an initial mechanistic model of interest, which can be further improved upon with neural network-based components to predict how the system will behave upon a wider range of conditions.[34-36]

Supporting Information

The authors have cited additional reference within the Supporting Information.^[37]

Research Article



15213773, 2025, 38, Downloaded from https://onlinelibrary.wiley.com/doi/10.1002/anie.202511413 by Cochrane Austria, Wiley Online Library on [07/11/2025]. See the Terms and Conditions (https://onlinelibrary.wiley.com/terms-and-conditions) on Wiley Online Library for rules of use; OA articless

are governed by the applicable Creative Commons License

Acknowledgements

Financial support from the Netherlands Organization for Scientific Research (to S.R.H., Grant No. OCENW.M.23.122) are acknowledged. Pieter van der Meulen is acknowledged for help with the NMR measurements. The authors thank the Center for Information Technology of the University of Groningen for providing access to the Hábrók High Performance Computing Cluster.

Conflict of Interests

The authors declare no conflict of interest.

Data Availability Statement

The data that support this study are available on GitHub at https://Github.Com/MLeCacheux/IterativeParamEst.

Keywords: Autocatalysis • CRNs • Kinetics • Modeling • Oscillations • Parameter estimation • Systems chemistry

- Y. Cao, A. Lopatkin, L. You, Nat. Struct. Mol. Biol. 2016, 23, 1030–1034.
- [2] M. Zhou, W. Wang, S. Karapetyan, M. Mwimba, J. Marqués, N. E. Buchler, X. Dong, *Nature* 2015, 523, 472–476.
- [3] X. Zheng, A. Sehgal, Genetics 2008, 178, 1147-1155.
- [4] D. Morse, P. Sassone-Corsi, *Trends Neurosci.* **2002**, 25, 632–637.
- [5] H. G. Mayr, J. H. Yee, M. Mayr, R. Schnetzler, Nat. Sci. 2012, 04, 233–244
- [6] B. Chance, A. K. Ghosh, E. K. Pye, In Biological and Biochemical Oscillators, Aufl., Johnson Research Foundation Colloquia, Vol. 1, Elsevier Reference Monograph: s.l, New-York 1973.
- [7] A. Goldbeter, Philos. Trans. R. Soc. Math. Phys. Eng. Sci. 2018, 376, 20170376.
- [8] L. Glass, Nature 2001, 410, 277-284.
- [9] H. Landolt, Berichte Dtsch. Chem. Ges. 1886, 19, 1317–1365.
- [10] B. P. Belousov, [Periodically Acting Reaction and Its Mechanism]. Сборник Рефератов По Радиационной Медицине, Vol. 147, Meditsina Publishers, Moscow 1959, pp. 145.
- [11] I. R. Epstein, J. A. Pojman, An Introduction to Nonlinear Chemical Dynamics: Oscillations, Waves, Patterns, and Chaos, Topics in Physical Chemistry, Oxford University Press, New York, 2020.
- [12] S. Hess, A. Mikhailov, Science 1994, 264, 223–224.
- [13] J. Boissonade, P. De Kepper, J. Phys. Chem. 1980, 84, 501–506.
- [14] M. Orbán, P. De Kepper, I. R. Epstein, K. A. Kustin, *Nature* 1981, 292, 816–818.
- [15] G. Rabai, M. Orban, I. R. Epstein, Acc. Chem. Res. 1990, 23, 258–263.

- [16] B. V. D. Pol, Lond. Edinb. Dublin Philos. Mag. J. Sci. 1926, 2, 978–992.
- [17] M. Orbán, K. Kurin-Csörgei, I. R. Epstein, Acc. Chem. Res. 2015, 48 593–601.
- [18] K. Kovacs, R. E. McIlwaine, S. K. Scott, A. F. Taylor, J. Phys. Chem. A 2007, 111, 549–551.
- [19] X. Li, P. Fomitskaya, V. A. Smaliak, B. S. Smith, E. V. Skorb, S. N. Semenov, *Nat. Commun.* 2025, 15, 3316.
- [20] A. I. Novichkov; A. I. Hanopolskyi, X. Miao, L. J. W. Shimon, Y. Diskin-Posner, S. N. Semenov, *Nat. Commun.* 2021, 12, 2994.
- [21] S. N. Semenov, L. J. Kraft, A. Ainla, M. Zhao, M. Baghbanzadeh, V. E. Campbell, K. Kang, J. M. Fox, G. M. Whitesides, *Nature* 2016, 537, 656–660.
- [22] M. G. Howlett, A. H. J. Engwerda, R. J. H. Scanes, S. P. Fletcher, Nat. Chem. 2022, 14, 805–810.
- [23] M. T. Harmsel, O. R. Maguire, S. A. Runikhina, A. S. Y. Wong, W. T. S. Huck, S. R. Harutyunyan, *Nature* 2023, 621, 87–93.
- [24] A. S. Leathard, P. A. Beales, A. F. Taylor, Chaos Interdiscip. J. Nonlinear Sci. 2023, 33, 123128.
- [25] M. Wen, E. W. C. Spotte-Smith, S. M. Blau, M. J. McDermott, A. S. Krishnapriyan, K. A. Persson, *Nat. Comput. Sci.* 2023, 3, 12–24.
- [26] S. Y. Wong, W. T. S. Huck, Beilstein J. Org. Chem. 2017, 13, 1486– 1497
- [27] E. Klipp, W. Liebermeister, C. Wierling, A. Kowald, Systems Biology: A Textbook, 2nd ed., Wiley-VCH, Weinheim 2016.
- [28] J. Pitt, J. Banga, BMC Bioinformatics 2019, 20, 82.
- [29] M. Gasparyan, S. Rao, Bioengineering 2023, 10, 1056.
- [30] T. O. E. Jones, P. Peterson, SciPy: Open Source Scientific Tools for Python 2001.
- [31] S. Hoops, S. Sahle, R. Gauges, C. Lee, J. Pahle, N. Simus, M. Singhal, L. Xu, P. Mendes, U. Kummer, *Bioinformatics* 2006, 22, 3067–3074
- [32] P. J. Shami, J. E. Saavedra, C. L. Bonifant, J. Chu, V. Udupi, S. Malaviya, B. I. Carr, S. Kar, M. Wang, L. Jia, X. Ji, L. K. Keefer, J. Med. Chem. 2006, 49, 4356–4366.
- [33] A. E. Maciag, J. E. Saavedra, H. Chakrapani, Anticancer Agents Med. Chem. 2009, 9, 798–803.
- [34] C. Rackauckas, Y. Ma, J. Martensen, C. Warner, K. Zubov, R. Supekar, D. Skinner, A. Ramadhan, D. Edelman, arXiv 2020, https://doi.org/10.48550/ARXIV.2001.04385.
- [35] M. Philipps, N. Schmid, J. Hasenauer, Universal Differential Equations for Systems Biology: Current State and Open Problems, December 5, 2024, https://doi.org/10.1101/2024.11.29. 626122.
- [36] M. De Rooij, B. Erdős, N. A. W. Van Riel, S. D. O'Donovan, PLoS Comput. Biol. 2025, 21, e1012198.
- [37] K. Gondo, J. Oyamada, T. Kitamura, Org. Lett. 2015, 17, 4778–4781.

Manuscript received: May 25, 2025 Revised manuscript received: July 09, 2025 Accepted manuscript online: July 24, 2025 Version of record online: August 06, 2025